NTU Hand: A New Design of Dexterous Hands

Li-Ren Lin*
Graduate Student.

Han-Pang Huang
Professor.

Robotics Laboratory, Department of Mechanical Engineering, National Taiwan University, Taipei, TAIWAN 10674, R.O.C.
hphuang@w3.me.ntu.edu.tw

A new five-finger robot hand (NTU hand) with seventeen degrees of freedom (DOF) is developed in this paper. In contrast to traditional tendon-driven robots, the NTU hand has an uncoupled configuration that each finger and joint are all individually driven. Since all actuators, mechanical parts and sensors are packed on the hand, the size of NTU hand is almost the same as a human hand. Such compact design makes the hand easily adapt to the industrial robot arm and the prosthetic applications. Based on the mechanical structure of the NTU hand, the direct and inverse kinematics are developed. In addition, computer simulation with three-dimension graphics is built to evaluate the manipulable range of the NTU hand. From the simulation, the relationship between the hand and the grasped object in a specific point of view can be obtained.*

1 Introduction

The operation of multifingered robot hands for fine motion and dexterous manipulation is an interesting topic in research and applications of robotics. The multifingered robot acts as a multipurpose gripping device for various tasks. Since it is designed to replace some work of human hands, most multifingered robots duplicate the shape and function of human hands. In order to manipulate various objects and tools, dexterity is the first requirement for the multifingered robots. In addition to the dexterous manipulation, the ability to perform power grasp is also required. The size of the hand is a significant part in research. A compact enough multifingered robot can be directly attached to the end of an industrial robot arm, or play a role in prosthetics.

Many multifingered robot hands have been developed. The number of fingers ranges from three to five. An example of three-fingered robot hand is the JPL/ Stanford hand (Stansfield, 1990, see Fig. 1). Each finger has three DOFs and is driven by four motors through tendon cables. Two parallel axis joints provide rotation and the third proximal joint, perpendicular to the other joints, provides the sideward motion. Due to large number of motors and strong coupling in the tendon configuration, the control system of JPL/ Stanford hand is very complicated. In addition, it is difficult to maintain calibration by using the tension of four cables in a finger.

The Utah/MIT hand (Jacobsen et al., 1984, see Fig. 2) has one thumb and three fingers. Each finger has four joints. Three parallel joints provide the rotation and the proximal joint supplies the lateral action. Due to the Utah/MIT hand has four DOFs in each finger, eight independent tendons and pneumatic cylinders are required. Each pair of tendons must keep tension to maintain the joint of the robot finger. Once a lateral motion is performed, one joint is activated and the other three joints keep stationary so that tensions on eight tendons must be recalculated. The coupling problem also causes the Utah/MIT hand to use large number of actuators and complex control system (Speeter, 1990). The above two fingered hands are bulky because of the tendon driven configurations and associated control systems.

The Belgrade/ USC hand (Tomovic et al., 1987, see Fig. 3) has five fingers and four motors, two motors for the thumb and two for the other fingers. Each finger has three parallel axis joints but only one DOF. The hand only provides simple grasping capacity rather than dexterous manipulation. The multifingered robot of Yaskawa Electric Corporation has three fingers and nine DOFs (Umetsu and Oniki, 1993). This hand only utilizes its fingertip because of the bulky cylinder finger segments. The above two hands are not suitable candidates for prosthetics.

In this paper, we propose a new approach to design and implement a dexterous artificial hand: NTU hand. The NTU hand is designed so that it is potential for both robotics and prosthetics applications. The outlook of the NTU hand is shown in Fig. 4. Due to the design of uncoupled mechanism, each finger and joints of the NTU hand are all individually driven. Hence, the dexterity of the NTU hand can be obtained from the uncoupled arrangement. The specifications and some issues of the mechanical consideration will be further stated. Based on the idea of design for manufacture and design for control, the kinematics of the NTU hand turn out to be simple. In particular, the inverse kinematics are unique. In addition, for further justifying the manipulable range of the NTU hand, 2D and 3D workspaces of the NTU hand are provided by a built-in posture monitor with three-dimension graphics. From the simulation, we can obtain the relation between the hand and the grasped object in a specific point of view.

This paper is organized into three parts: mechanism design, kinematics and simulations. Finally, the conclusions are made.

2 Mechanism Design

Many multifingered hands are driven by tendon cables. One reason is that cables act as muscles of human hands. Another reason is that actuators, reduction gears and sensors can be remotely installed to keep the hand itself compact. However, all traditional hands suffer from bulky mechanism and are inconvenient for practical applications. In this paper, a modular design is proposed to design the NTU multifingered robot hand so that its driven mechanism is uncoupled and its size is good for both industrial and prosthetic applications.

Our goals of the mechanism design are several folds. The first goal aims to the functionality purpose; i.e., numbers of fingers and DOFs. It is known that three hard fingers are required for a force closure grasp of a 2-D object, and four fingers are required to grasp a 3-D object (Markenscoff et al., 1990). Although the number of fingers can be reduced by one with suitable, realistic model of the fingertip under the same conditions (Mirtich and Canny, 1994), a human hand is always the design goal.

The second goal is the size. The hand including the overall driven mechanism should be about the same size as the human

* The NTU hand holds a patent with number 107115 in R.O.C.

Contributed by the Mechanisms Committee for publication in the JOURNAL OF MECHANICAL DESIGN. Manuscript received Jan. 1996. Associate Technical Editor: B. Ravani.

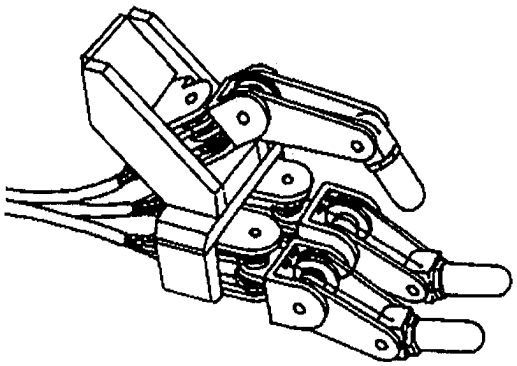

Fig. 1 The Standford/JPL hand

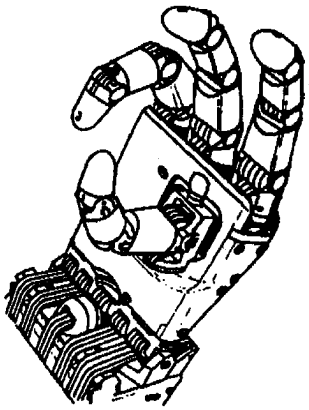

Fig. 2 The Utah/MIT hand

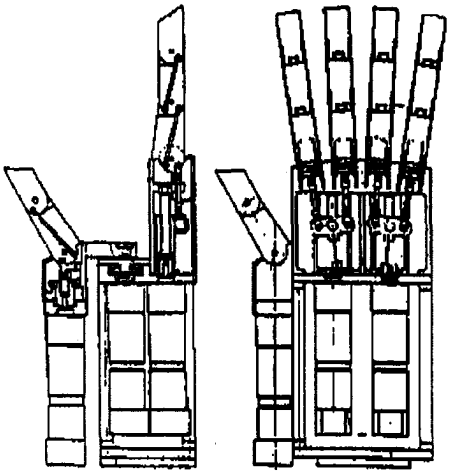

Fig. 3 The Belgrade/USC hand

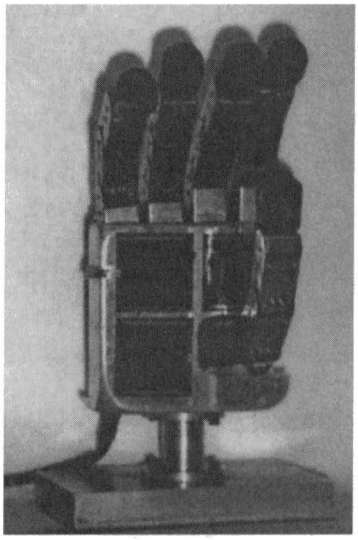

Fig. 4 The NTU hand

hand. Limitation of the size makes the hand suitable for robotics and rehabilitation applications. Once all parts are packed in the hand itself, the hand can be easily attached to the wrist of an industrial robot or the casualty.

The next goal focuses on the fabrication and maintenance. If the same parts can be repeatedly used in the modular design of the hand, the number of types of parts will be reduced and the cost will be down. Once the fingers are independent and exchangeable, the maintenance simply means to replace the damaged finger assembly without recalibration of the whole system.

The last goal deals with the potential of improvement. The performance can be enhanced by replacing the parts whenever better materials are available. But, the main design is preserved. Once the materials of transmission or the power of actuators are improved, the performance of the hand is also enhanced.

Based on the above design goals, the NTU hand has five fingers with seventeen DOFs. Both thumb and the first finger have four joints; two at knuckle, one between proximal and middle finger segments, and one between middle and distal finger segments. Other fingers have three joints; but only one at knuckle. Each finger is equipped with tactile sensors to detect grasping force. Due to cost issue and practical implementation,

Nomenclature

$^{j}T_i^f$ = the D-H transformation matrix of f-th finger for adjacent frames i and j

$\mathbf{x}_j$ $\mathbf{y}_j$ $\mathbf{z}_j$ = the axes of the coordinate frame j

θ_j = the joint angle from the $\mathbf{x}_{j-1}$ axis to $\mathbf{x}_j$ axis about the axis $\mathbf{z}_{j-1}$ (using the right-hand rule)

d_j = the distance from the origin of the $(i-1)$th coordinate frame to the intersection of the $\mathbf{z}_{j-1}$ axis with the $\mathbf{x}_j$ axis along the $\mathbf{z}_{j-1}$ axis

a_j = the shortest distance between the $\mathbf{z}_{j-1}$ and $\mathbf{z}_j$ axes

α_j = the offset angle from the $\mathbf{z}_{j-1}$ to the $\mathbf{z}_j$ axes along the $\mathbf{x}_j$ axis (using the right-hand rule)

θ_j^f = the joint angle of the joint j of the f-th finger

$\mathbf{n}_i^{f\alpha}$ = the normal vector ($\mathbf{x}_\alpha$) of coordinate frame α of the f-th finger with respect to the coordinate frame i of the f-th finger

$\mathbf{s}_i^{f\alpha}$ = the sliding vector ($\mathbf{y}_\alpha$) of coordinate frame α of the f-th finger with respect to the coordinate frame i of the f-th finger

$\mathbf{a}_i^{f\alpha}$ = the approach vector ($\mathbf{z}_\alpha$) of coordinate frame α of the f-th finger with respect to the coordinate frame i of the f-th finger

$\mathbf{p}_i^{f\alpha}$ = the position vector of coordinate frame α of the f-th finger with respect to the coordinate frame i of the f-th finger

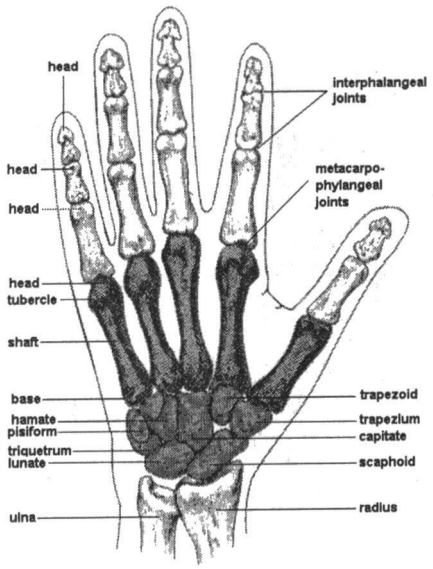

Fig. 5 The human hand

the tactile sensors are attached to the inner sides of finger segments and the palm, as shown in Fig. 4. We will present the concept and design details in the subsequent sections.

2.1 Hand Mechanism. The idea of design is obtained from the human hand. Since the structures of the fingers of human hand are almost the same and independent, as shown in Fig. 5, this feature gives us the idea to design the hand beginning with finger and to simplify the development. The human finger consists of finger segments. This fact also gives us the inspiration to design an independently driven finger segment and thus construct a complete finger. The auxiliary devices for the artificial finger are also required for the lateral motion, as the function of muscles in the palm.

2.1.1 The Finger and the Finger Segment. The finger of the NTU hand consists of distal segment, middle segment, proximal segment and base finger segment. To ease the manufacture and assembly, the group technology is applied to the design of the fingers and finger segments. The design should avoid the coupling problem of tendon driven structure and limit the size to make it easy for applications. Since we use modular design, each finger is composed of finger segments, as shown in Fig. 6. Once an individual finger is constructed, the mechanism of the whole robot hand is almost complete. In order to meet the requirement of the independently driven, it is essential to design a finger with all equipped parts.

The finger design is shown in Fig. 7. Each finger segment, except the distal segment, contains one high performance micro motor that drives a set of specially arranged gear trains to rotate the previous finger segment, as shown in Fig. 8. The gear ratio of the middle and proximal finger segments is about one hundred, but the gear ratio of the base segment is about one thousand for the sake of heavy load. The position sensor of each joint is installed in each finger segment. It is driven by the gear within the gear trains, and is proportional to the angle of the finger joint.

There are many electrical wires in the inner space of each segment shell, the placement of sensors and motors must be taken into account during the assembly process. Since the position sensor is driven by gear within the gear trains, its calibration must be accomplished during the assembly process.

2.1.2 The Auxiliary Device for the Lateral Joints. To ease the manufacture effort, the lateral rotation of the thumb and the first finger is achieved by adding auxiliary device to a fundamental finger, and the mechanic power is provided by an additional finger segment. The auxiliary devices of the thumb and the first finger are shown in Fig. 9. In the design of the lateral joint of the thumb, we attach a large gear to the thumb and use a modified finger segment to drive it. In the design of the lateral joint of the first finger, we use an adjustable linkage with a ball joint to transfer the mechanic power; i.e., they convert the rotation of the gear into the linear motion. The thumb and the first finger, each with four DOFs, provide approximately anthropomorphic motions similar to the natural human hand.

2.1.3 The Palm and the Wrist. The palm serves as a structural mounting base for the thumb, fingers and the wrist. The last three fingers are fixed on the palm by a board that arranges the fingers to cooperate with the thumb and the first finger. The upper space of the palm provides the location to install the controller and various electronic components (Huang and Lin, 1995). The overall design scheme of the NTU hand is shown in Fig. 12. The wrist shown in the scheme is designed to connect the NTU hand to the robot arm PUMA 560. Once the design of the NTU hand is modified for rehabilitation purpose, the wrist needs to be changed to adapt to the casualty.

2.1.4 The Tactile Sensors. One of the important sensing of the human hand is the tactility. An multifingered hand needs to equip tactile sensors for detecting contact force. Based on the consideration of contact possibility, cost, and practical implementation, the tactile sensors are attached to the finger tips, the inner sides of finger segments and the palm, as shown in Fig. 10. The palm and each finger of the NTU hand are equipped with tactile sensors to detect grasping force, as shown in Figs. 4 and 6. Each tactile sensor is calibrated to cooperate with the hardware of the control, as shown in Fig. 11.

2.2 Specifications of the Prototype. Since the fundamental finger of the NTU hand has three joints, numbered from 1 to 3, the specifications of the three joints of each finger are all

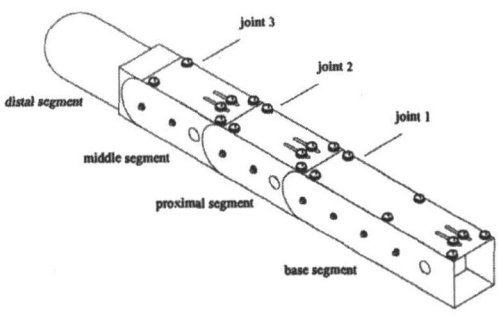

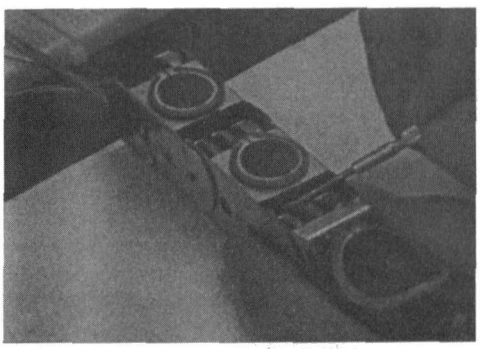

Fig. 6 The fundamental finger of the NTU hand

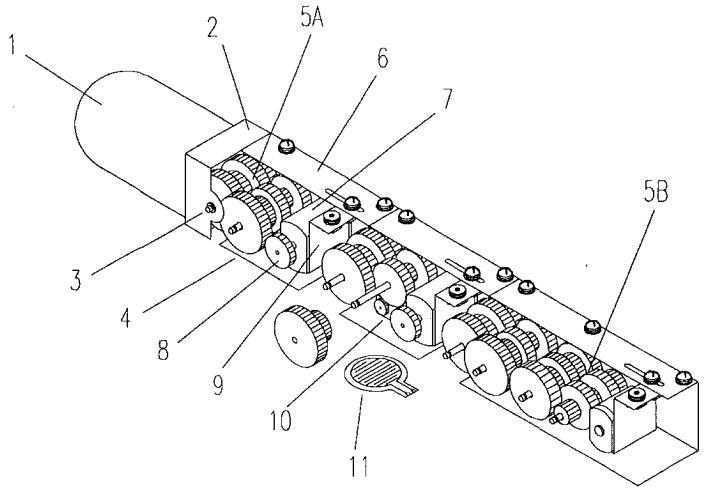

1. The finger tip	6. The cover of the finger segment
2. The base of the finger tip	7. The high performance micro motor
3. The Shaft	8. The gear on the shaft of motor
4. The Shell of the finger segment	9. The seat of the motor
5A. The Gear train A (96:1)	10. The position sensor
5B. The Gear train B (812:1)	11. The tactile sensor

Fig. 7 The assembly of the fundamental finger

the same. The lateral joints (joint 0) of the thumb and the first finger are performed by different auxiliary devices. The specifications of these two joints are special.

The specifications of the NTU hand are listed in Table 1. The prototype of the NTU hand is made of metal. Its weight can be reduced when other materials are used. The rated weight of the object to be manipulated dynamically is determined by dexterous operation while the object is operated by fingertips of the hand. The rated weight of the object to be grasped statically is determined by power grasp operation while the object is grasped by fingertips and inner links of the fingers and palm of the hand.

2.3 Verification and Improvement. In this section, the design goals of the hand are closely verified. We also discuss the problems that should be improved in next generation of the NTU hand.

2.3.1 Satisfactions of the Goals. As mentioned before, there are at least four goals to be qualified.

The Functionality Purpose. The NTU hand has five fingers with seventeen DOFs. All fingers have three parallel joints. The thumb and the first finger have additional joints to perform lateral motion. All existing hands use at least three dexterous fingers to grasp, while the NTU hand uses the middle finger to cooperate with the dexterous thumb and the first finger. This design makes the hand be simple and also achieve the most degree of manipulability. The last two fingers of the NTU hand are used to improve the stability of object holding.

Based on the above discussion, the all five fingers of the NTU hand have the functional duty. From a decoration point of view, the five-finger design resembles a human hand. In addition, the NTU hand with a glove of artificial skin can be used for prosthetic applications.

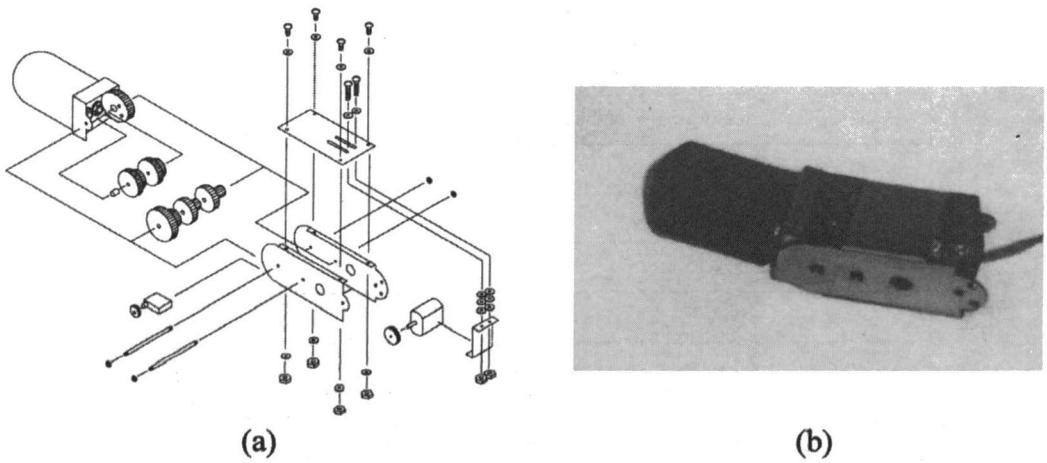

Fig. 8 The assembly of the distal segment and middle segment

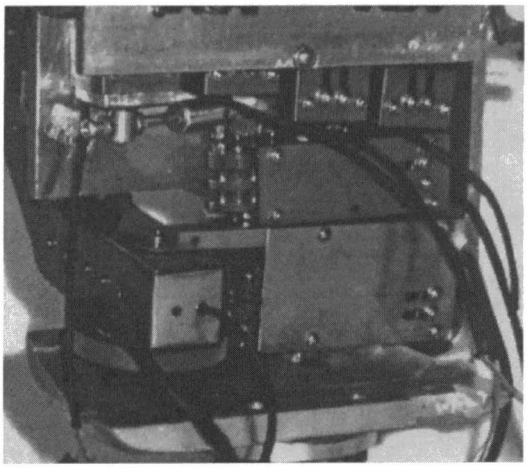

Fig. 9 The auxiliary device for the lateral joints of the thumb and first finger

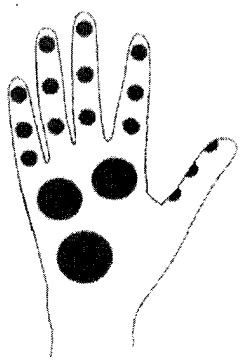

Fig. 10 Locations of the tactile sensors

The Required Space. From the mechanism design of the NTU hand, we can find the mechanical parts are all packed inside the hand itself. The size of the hand is very compact in terms of the mechanism point of view. However, The essential requirements of the artificial hand are not just the mechanism. They include electronic parts, such as controller, interface, power supply and so on.

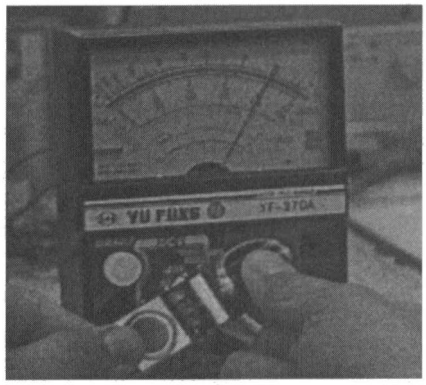

Fig. 11 Calibration of the tactile sensors

The specially designed controller is also built to satisfy the space limitation (Lin and Huang, 1995). The analog controllers perform the joint control and feedback the joint position. We also implement the compact analog controllers as shown in Fig. 13(a). Each analog controller module contains two controllers to output the control efforts to motors. Figure 13(b) is the signals distribution board which has nine slots to connect to the analog controller modules. The digital controller also has a slot to connect to the signals distribution board, as shown in Fig. 13(c). Once the controller boards are connected and stacked, it can mount on the back of the NTU hand (as the top of Fig. 12). The size of the controller is also compact.

It is clear that the mechanical and electronic parts are integrated into the NTU hand itself and occupy small space. This also explains why the NTU hand is suitable for prosthetic application.

Effort of the Fabrication and Maintenance. As shown in the Fig. 7 and Fig. 12, most of the same parts in the finger segments are repeatedly used. The modular design not only lowers down the fabrication cost but eases the maintenance efforts.

The Potential of Improvement. The most efficient way to improve the performance of the hand is to change the materials

Table 1 The specifications of prototype of the NTU hand

	Joint 0 of the thumb	Joint 0 of the first finger	Joint 1 of each finger	Joint 2 of each finger	Joint 3 of each finger
maximum angular velocity	0.21 rad/s	0.39 rad/s	1.05 rad/s	5.97 rad/s	7.33 rad/s
bandwidth	0.15 Hz	0.31 Hz	0.50 Hz	2.85 Hz	3.50 Hz
torque output	3661.9 g-cm	1971.8 g-cm	1350.1 g-cm	859.44 g-cm	859.44 g-cm
The weight of each finger				191.2 g	
The weight of the palm and auxiliary device				613.1 g	
The total weight of the NTU hand				1569.0 g	
The rated weight of the object to be manipulated dynamically				0.5 Kg	
The rated weight of the object to be grasped statically				1.0 Kg	
The maximum linear velocity of finger tip				877.08 mm/s	
The current consumption of the whole hand mechanism				0A - 8.5A	

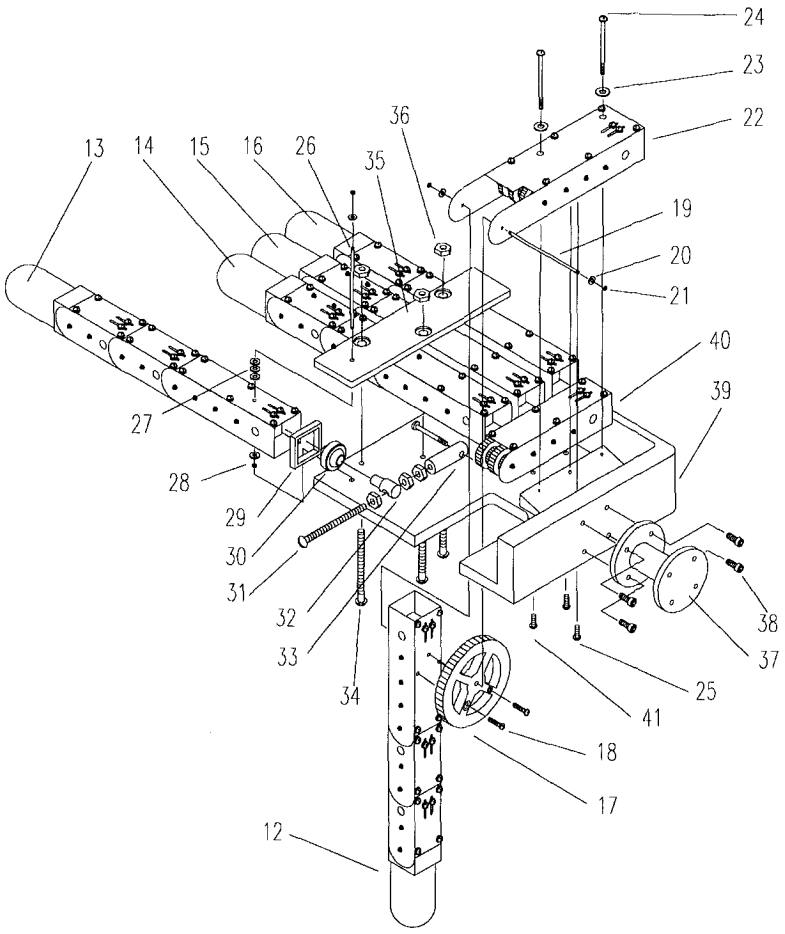

12. The thumb	22. The modified finger segment	32. The shaft of the ball bearing
13. The first finger	23. The washer	33. The nut of the adjust bolt
14. The middle finger	24. The bolt	34. The bolt of the part 35
15. The ring finger	25. The bolt	35. The board to fix the last three fingers
16. The little finger	26. The lateral shaft of the first finger	36. The nut of the part 35
17. The lateral gear on the thumb	27. The washers	37. The wrist to adapt robot arm
18. The bolt	28. The E ring	38. The nut to connect palm
19. The lateral shaft of the thumb	29. The rectangle frame	39. The palm
20. The washer	30. The ball bearing	40. The finger segment for the lateral movement of the first finger
21. The E ring	31. The adjust bolt with screw	

Fig. 12 The assembly of the NTU hand

of the hand. The selection of the material depends on the application of the hand. The prototype of the NTU hand, as shown in Fig. 4, is built by steel and aluminum except the polymer fingertips. The weight of the hand, which is appropriate for robotics applications, is listed in Table 1. Due to the compact size of the whole system, the high possibility for prosthetic applications is one advantage of the NTU hand. For the prosthetic applications, the material can be chosen to reduce the

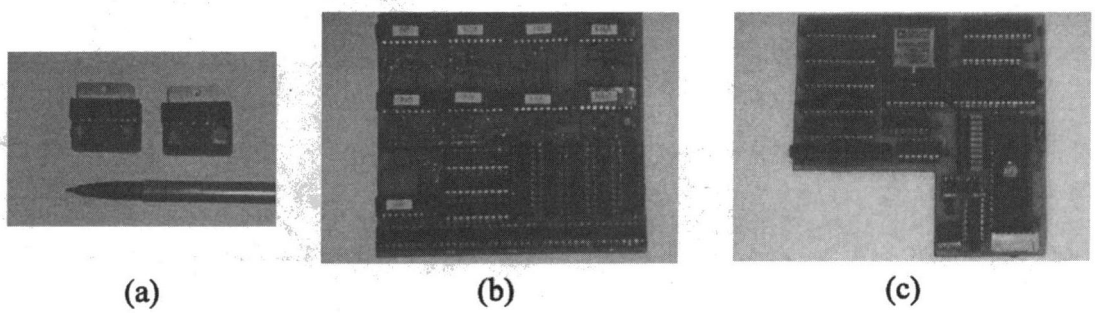

Fig. 13 Hardware of the controller

weight without decreasing the strength. It may be some polymer or composite material. The material of the hand can be chosen in terms of different applications, but the design spirit of the hand will not change, or just slight modifications.

2.3.2 Problems of the Present Design. The present design suffers from some problems. These problems determine the performance of the NTU hand. This sub-section states what problems we encounter in the present design and how we solve.

Problem of the Gear Driven. The driven mechanism of the NTU hand is performed by a set of gear trains. The disadvantage of the gear driven is the backlash problem. It means that the accuracy of the joint position will not be good. The problem is not serious while the hand is operated to grasp objects. The backlash will not happen because the gears are keeping contact during the grasp operation. The most important is the tactile sensing while grasping.

The sensing of the NTU hand is divided into two parts, one is the joint variables, the other is the tactile sensing. According to the grasp of the human, the posture of the hand is not very accurate because the main goal of grasp is to manipulate an object. It means that the function of the finger movement is keeping in contact with the object. The design of the NTU hand also follows the guide line that the tactile sensing is the first consideration and then movement of the finger joint. It also implies that we can reduce the cost in the hand design.

Force, Torque and Heat Sink. The torque output of the finger segment is high because of the high gear ratio. Hence, the force of the hand will be large. The limitation of the force output is determined by the capacity of motors and the strength of gears. The modulus and thickness of the final stage of the gear trains should be larger than the pervious stage to stand the larger torque. Alternatively, we may use the high strength gear in the final stage of the gear trains.

The heat sink of the motor is also related to the force output. The torque of the motor decreases while the heat accumulates in the chamber of the finger segment. In the prototype of the NTU hand, we use a seat (part 9 in the Fig. 7) of motor to transfer the heat to the outside of the finger segment.

Since the electronic amplifiers of the analog controllers are stacked on the top of the controller, as shown in Fig. 13, its location is on the top of Fig. 12. The heat sink of the electronic amplifier can use the back cover of the NTU hand. It means the heat can be directly delivered to the shield of the hand for efficient dissipation of heat.

3 Kinematics

3.1 Direct Kinematics. The coordinate frames of the NTU hand are shown in Fig. 14. Note that the thumb and the first finger have four joints, numbered from 0 to 3; and the rest of three fingers only have three joints, numbered from 1 to 3. In the derivation of inverse kinematics for the NTU hand, each finger is treated the same as the thumb or the first finger, except the joint 0. The link parameters of each finger are listed in Table 2, based on Denavit-Hartenberg (1955) method. The matrix ${}^{j-1}T_j^f$ is known as the D-H transformation matrix for adjacent frames, j and $j-1$. Thus,

Table 2 The link parameters of finger (*for thumb, !for first finger)

	θ_j (degree)	α_j (degree)	a_j (mm)	d_j (mm)	joint range (degree)
joint 0*,!	0	90	35.2 *,!	0	-30~45 * -10~10 !
joint 1	0	0	34.0	0	0~60
joint 2	0	0	34.0	0	0~60
joint 3	0	0	42.0	0	0~60

$$ {}^{j-1}T_j^f = \begin{bmatrix} \cos\theta_j & -\cos\alpha_j \sin\theta_j & \sin\alpha_j \sin\theta_j & a_j \cos\theta_j \\ \sin\theta_j & \cos\alpha_j \cos\theta_j & -\sin\alpha_j \cos\theta_j & a_j \sin\theta_j \\ 0 & \sin\alpha_j & \cos\alpha_j & d_j \\ 0 & 0 & 0 & 1 \end{bmatrix} \tag{1} $$

The homogeneous matrix ${}^{base}T_j^f$, which specifies the location of the j-th coordinate frame of the f-th finger with respect to the finger base of the coordinate system, is the chain product of successive ${}^{j-1}T_j^f$, and is expressed as

$$ {}^{base}T_3^f = {}^{base}T_0^f \, {}^0T_1^f \, {}^1T_2^f \, {}^2T_3^f = \begin{bmatrix} \mathbf{n}_{base}^{f3} & \mathbf{s}_{base}^{f3} & \mathbf{a}_{base}^{f3} & \mathbf{p}_{base}^{f3} \\ 0 & 0 & 0 & 1 \end{bmatrix} \tag{2} $$

$$ {}^0T_3^f = {}^0T_1^f {}^1T_2^f {}^2T_3^f = \begin{bmatrix} \mathbf{n}_0^{f3} & \mathbf{s}_0^{f3} & \mathbf{a}_0^{f3} & \mathbf{p}_0^{f3} \\ 0 & 0 & 0 & 1 \end{bmatrix} \tag{3} $$

where

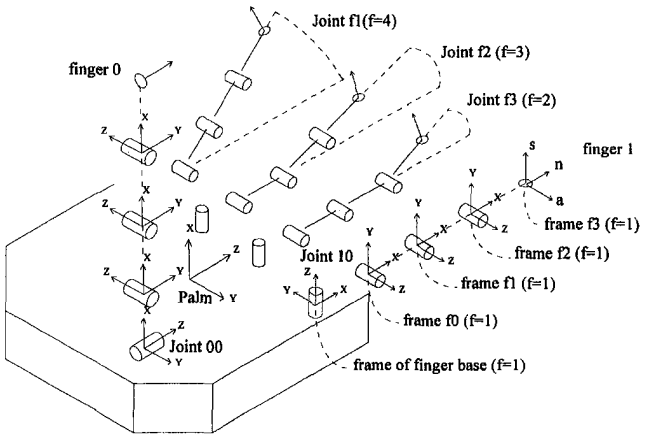

Fig. 14 The coordinate frame of the NTU hand

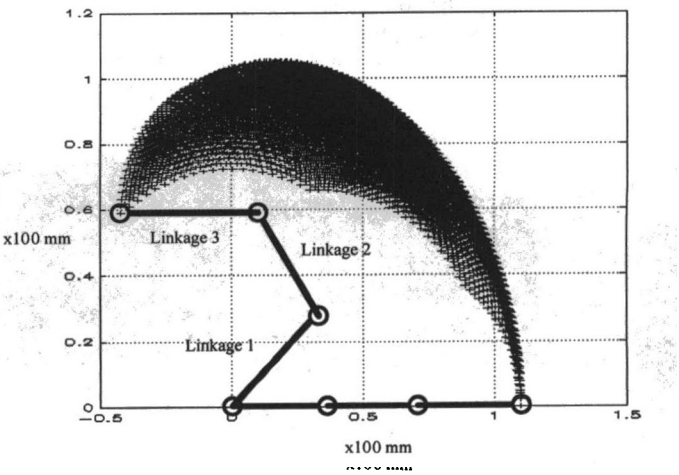

Fig. 15 The workspace of the finger

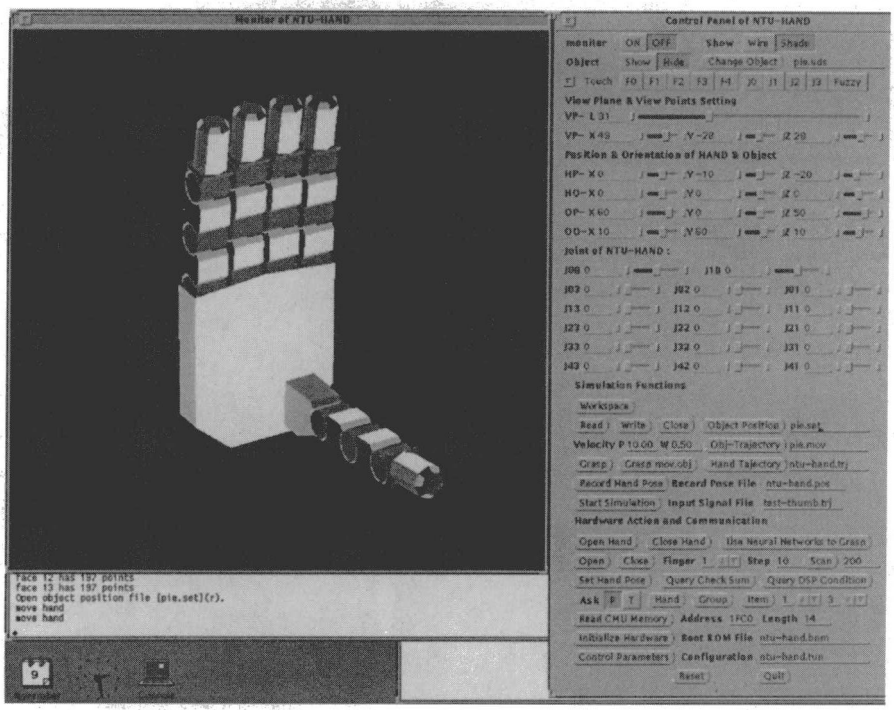

Fig. 16 The 3D user interface

$$\mathbf{n}_i^{f\alpha} = \begin{bmatrix} n_{i,x}^{f\alpha} \\ n_{i,y}^{f\alpha} \\ n_{i,z}^{f\alpha} \end{bmatrix}, \quad \mathbf{s}_i^{f\alpha} = \begin{bmatrix} s_{i,x}^{f\alpha} \\ s_{i,y}^{f\alpha} \\ s_{i,z}^{f\alpha} \end{bmatrix}, \quad \mathbf{a}_i^{f\alpha} = \begin{bmatrix} a_{i,x}^{f\alpha} \\ a_{i,y}^{f\alpha} \\ a_{i,z}^{f\alpha} \end{bmatrix}$$

$$\text{and} \quad \mathbf{p}_i^{f\alpha} = \begin{bmatrix} p_{i,x}^{f\alpha} \\ p_{i,y}^{f\alpha} \\ p_{i,z}^{f\alpha} \end{bmatrix}, \quad \alpha = 1, 2, 3$$

Upon assigning the joint variables of f-th finger, the corresponding transformation matrices ${}^{\text{base}}T_3^f$ and ${}^0T_3^f$ can be found. For the configuration of the NTU hand, the matrix ${}^0T_3^f$ is determined by joints 1, 2, 3 for all fingers. Notice that the matrix ${}^{\text{base}}T_3^f$ is a function of joint 0 as dealing with the thumb and the first fingers.

The orientation and position of each finger tip can be obtained from Eqs. (2) ~ (3). The normal vector $\mathbf{n}_i^{f3}$, sliding vector $\mathbf{s}_i^{f3}$ and approach vector $\mathbf{a}_i^{f3}$ determine the orientation of the finger tip with respect to the coordinate system i. The position vector $\mathbf{p}_i^{f3}$ represents the spatial shift between the finger tip and the origin of the i-th coordinate frame.

3.2 Inverse Kinematics. The inverse kinematics is derived from a known set of admissible vectors $\mathbf{n}_{\text{palm}}^{f3}$ and $\mathbf{p}_{\text{palm}}^{f3}$, then is transformed into $\mathbf{n}_{\text{base}}^{f3}$ and $\mathbf{p}_{\text{base}}^{f3}$ by homogeneous matrix ${}^{\text{palm}}T_{\text{base}}^f$. Hence, the θ_0^f (joint 0) of the finger can be obtained from the following equation,

$$\theta_0^f = \text{atan } 2(\mathbf{p}_{\text{base},y}^f, \mathbf{p}_{\text{base},x}^f) \tag{4}$$

where atan $2(y, x)$ returns $\tan^{-1}(y/x)$ with proper quadrant.

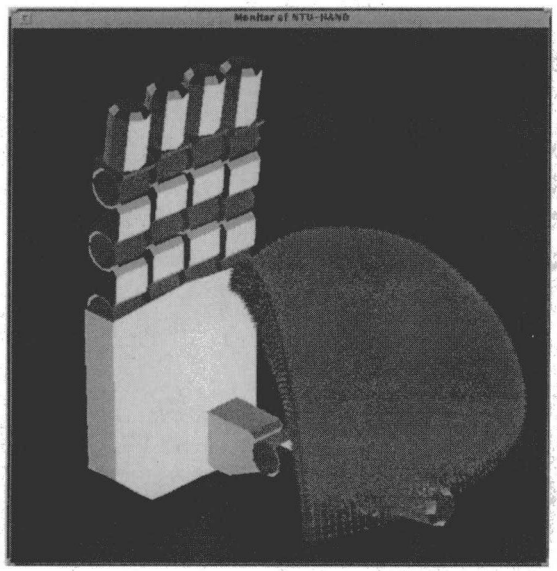

Fig. 17 The fingertip workspace of the thumb

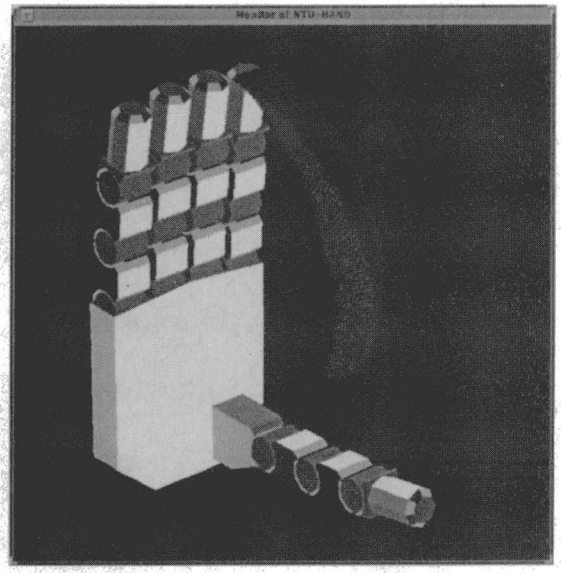

Fig. 18 The fingertip workspace of the first finger

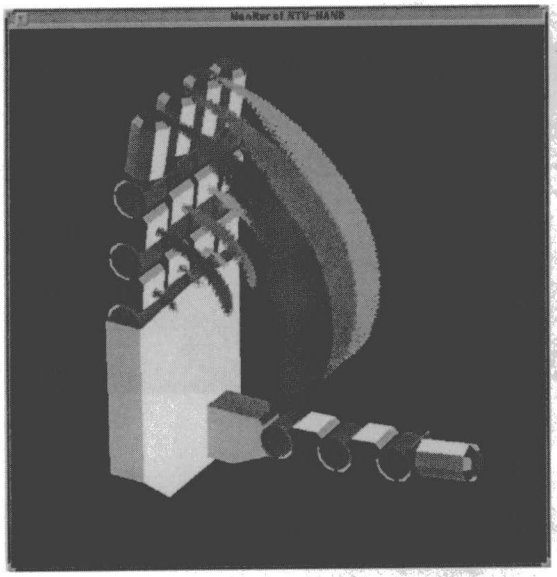

Fig. 19 The fingertip and segment workspaces of the last three fingers

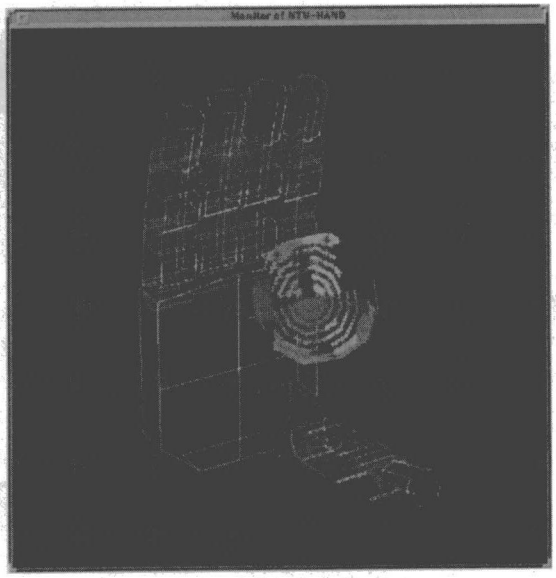

Fig. 21 The dedicated contact points on the object

To match the structure of the NTU hand, the following conditions must be satisfied,

$$\theta_0^f = 0 \quad \text{for} \quad f = 2, 3, 4 \tag{5}$$

From a known θ_0^f, we can find the corresponding $\mathbf{n}_0^{f3}$ and $\mathbf{p}_0^{f3}$ by homogeneous matrix ${}^0T_{6\text{base}}^f$. The derivation of the remaining joints is the same for all fingers. The inverse kinematics are shown below. Let

$$\theta_s^f = \theta_1^f + \theta_2^f + \theta_3^f = \text{atan } 2(n_{0,y}^{f3}, n_{0,x}^{f3}) \tag{6}$$

Define $p_x^f = p_{0,x}^{f3} - a_3 \cos \theta_s^f$ and $p_y^f = p_{0,y}^{f3} - a_3 \sin \theta_s^f$. Then, we have

$$\theta_1^f = \text{atan } 2(p_y^f, p_x^f) - \cos^{-1}\left(\frac{(p_x^f)^2 + (p_y^f)^2 + (a_1)^2 - (a_2)^2}{2a_1\sqrt{(p_x^f)^2 + (p_y^f)^2}}\right) \tag{7}$$

$$\theta_2^f = \pi - \cos^{-1}\left(\frac{(a_1)^2 + (a_2)^2 - (p_x^f)^2 - (p_y^f)^2}{2a_1a_2}\right) \tag{8}$$

$$\theta_3^f = \theta_s^f - \theta_1^f - \theta_2^f \tag{9}$$

If a set of points and corresponding normal vectors are calculated in terms of the above equations, and the solution of joint variables satisfies Table 2, we claim that there exists an admissible joint solution of a finger for the pair of point and normal vector. Due to the configuration of the NTU hand, the number of solutions generated by the inverse kinematics is only one. It is obvious because the ranges of joints 1, 2, 3 are limited within 60 degrees (Huang and Lin, 1995).

3.3 Workspace of the Finger. The dexterous workspace of one finger is shown in Fig. 15, which is obtained by direct kinematics. The dimension of the i-th linkage is the same as a_j in Table 2. Namely, the lengths of the linkage 1 and linkage 2 are 34 mm. The length of the linkage 3 is 42 mm. Notice that the density of marks shows the degree of dexterity of the finger-

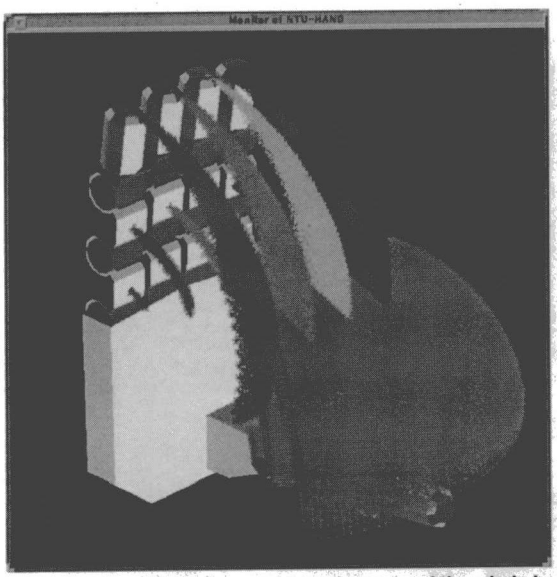

Fig. 20 The fingertip and segment workspaces of the whole hand

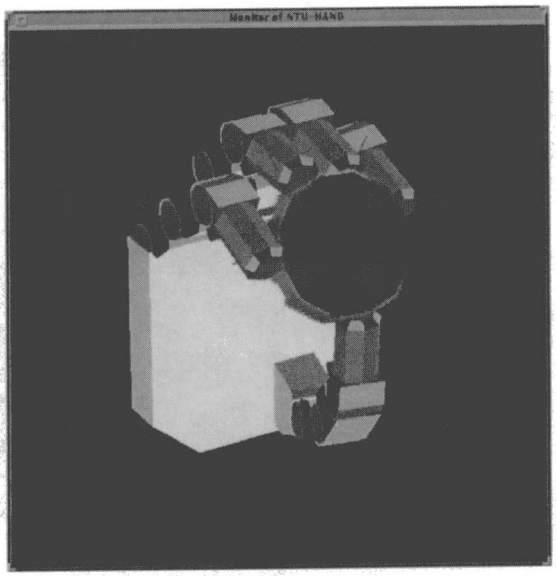

Fig. 22 The postures for grasping disc object

Table 3 The results of the workspace analysis (The increment of joints for θ_0^f to θ_3^f are 0.016, 0.063, 0.063 and 0.063 radian in the joint range of Table 2. The increment of the workspace scanning is 5 mm. Notice that the above notations of the axes are the same as Fig. 14.)

	The thumb (F=0)	The first finger (F=1)	The middle finger (F=2)	The ring finger (F=3)	The little finger (F=4)
workspace of the finger tip (J=3)					
volume (mm^3)	447625	40499	3374	3374	3374
number of points	280124	52250	20125	20125	20125
max. x (mm)	160	110	110	110	110
min. x (mm)	20	15	15	15	15
max. y (mm)	125	45	10	-10	-35
min. y (mm)	-50	30	10	-10	-35
max. z (mm)	80	160	165	165	160
min. z (mm)	-15	20	25	25	25
workspace of the middle finger segment (J=2)					
volume (mm^3)	55625	2699	2500	2500	2500
number of points	18674	5875	224	224	224
max. x (mm)	100	55	55	55	55
min. x (mm)	50	15	15	15	15
max. y (mm)	80	40	10	-10	-35
min. y (mm)	-20	30	10	-10	-35
max. z (mm)	25	100	105	105	105
min. z (mm)	-15	65	70	70	70
workspace of the proximal finger segment (J=1)					
volume (mm^3)	7625	500	500	500	500
number of points	1244	179	14	14	14
max. x (mm)	65	20	20	20	20
min. x (mm)	50	10	10	10	10
max. y (mm)	60	35	10	-10	-35
min. y (mm)	0	35	10	-10	-35
max. z (mm)	-10	65	70	70	70
min. z (mm)	-20	60	65	65	65

tip. The thumb and the first finger have more dexterity for the sake of the lateral joint. They expand the plane workspace of Fig. 15 into three dimensional spaces, as shown in the computer simulations of the next section. If each contact point lies in the workspace and a corresponding inverse kinematics can be found, the multifingered robot hand can perform a dexterous manipulation.

4 Computer Simulations

Since it is difficult to numerically interpret the posture of the multifingered hand with seventeen joint variables and the relationship with the grasped object, we design a 3D graphic interface for the simulation, as shown in Fig. 16. The simulation is performed on a SUN sparc 10 workstation under the *X* environment. The user can define the positions and orientations of the object and the hand, then set the grasp posture of the NTU hand. The relation between the hand and the object can be viewed from any angles.

Since the thumb and the first finger have the lateral joint in the base segment, they expand the plane workspace of Fig. 15 into three dimensions. Our 3D graphic user interface can also view the workspace in a specific view point. The workspace of the thumb is shown in Fig. 17. It looks like a shell. The workspace of the first finger is shown in Fig. 18. It is wide on the top and narrow on the bottom. Both sides of the workspaces of the thumb and the first finger are the same as Fig. 15. Fig. 19 shows the workspaces of the last three fingers, including the fingertip and the finger segments. We can also find the plane workspace in the three dimensional spaces. Figure 20 shows the workspace of the whole NTU hand. From this simulation result, we can find the intersection of the workspaces. They are the location at which fingertips are touched together.

Table 3 lists the results of the workspace analysis. The increments of joints for θ_0^f to θ_3^f are 0.016, 0.063, 0.063 and 0.063 radians in the joint range of Table 2. The increment of the workspace scanning is 5 mm. Based on the above setting, the numbers of points of workspaces are listed in the table. The corresponding volume, maximum and minimum workspaces can be determined from the simulation results.

After the relationship between the hand and the object is determined, the corresponding posture can be set in our simulation. Figure 21 shows the dedicated contact points on the object. The markers on the object are obtained from the intersection of the workspaces of the hand and surface of the object. Figure 22 shows the posture of the hand. The contact points on the object and the corresponding posture are chosen by the algorithm we provide (Lin and Huang, 1994). The cases of rectangular object and cylindrical object are also shown in Fig. 23–24.

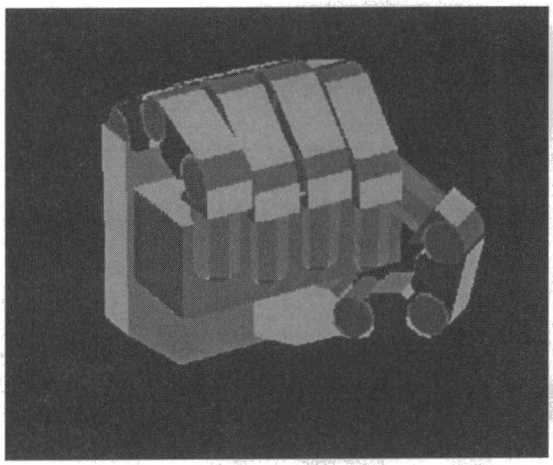

Fig. 23 The postures for grasping rectangular object

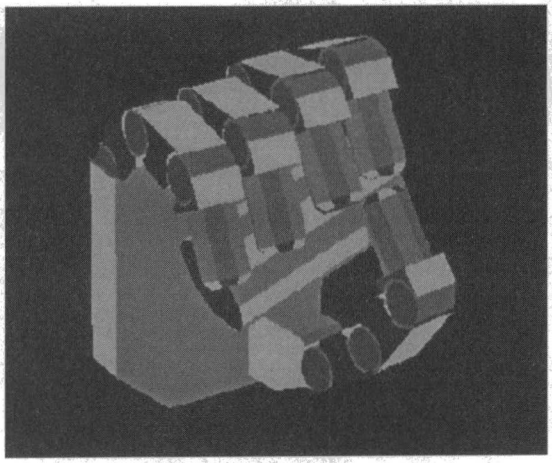

Fig. 24 The postures for grasping cylindrical object

5 Conclusions

The multifingered robot hand, NTU hand, with seventeen degrees of freedom has been designed and fabricated to achieve dexterous manipulation. Since the NTU hand is lighter and much more compact than traditional fingered hands and with an uncoupled driven mechanism, it can be easily attached to the end of a robot arm to perform dexterous manipulation. In particular, it is useful for prosthetic applications. According to the mechanical structure of the NTU hand, the specifications, the kinematics, workspace analysis and computer simulation for evaluation are also presented in this paper.

Acknowledgment

This research is partially supported by National Science Council of R.O.C. under Grant number NSC 84-2212-E002-032.

References

Denavit, J., and Hartenberg, R. S., 1955, "A Kinematics Notation for Low-Pair Mechanism Based on Matrices," ASME *Journal of Applied Mechanics,* pp. 215–221.

Fowler, I., 1984, *Human Anatomy,* Wadsworth Publishing, Belmont, California, pp. 155.

Huang, H. P., and Lin, L. R., 1995, "Development of A Prosthetic Hand with Multifingers," NSC Report, NSC 84-2212-E002-032.

Jacobsen, S. C., Wood, J. E., Knutti, D. F., and Biggers, K. B., 1984, "The UTAH/MIT Dextrous Hand: Work in Progress," *International Journal of Robotics Research,* Vol. 3, No. 4, pp. 21–50.

Lin, L. R., and Huang, H. P., 1994, "Use Hopfield Networks to Find A Grasping Solution for A Dextrous Hand," *IEEE International Symposium on Artificial Neural Networks,* pp. 716–721.

Lin, L. R., and Huang, H. P., 1995, "DSP-Based Fuzzy Control of A Multifingered Robot Hand," *IEEE International Conference on Systems, Man and Cybernetics,* pp. 3672–3677.

Markenscoff, X., Ni, L., and Papadimitriou, C. H., 1990, "The Geometry of Grasping," *International Journal of Robotics Research,* Vol. 9, No. 1, pp. 61–74.

Mirtich, B., and Canny, J., 1994, "Easily Computable Optimum Grasps in 2-D and 3-D," *IEEE International Conference on Robotics and Automation,* pp. 739–747.

Speeter, T. H., 1990, "Control of the Utah/MIT Dextrous Hand: Hardware and Software Hierarchy," *Journal of Robotics Systems,* Vol. 7, No. 5, pp. 759–790.

Stansfield, S. A., 1990, "Knowledge-based Robotic Gasping," *IEEE Conference on Robotics and Automation,* pp. 1270–1275.

Tomovic, R., Bekey, G. A., and Karplus, W. J., 1987, "A Strategy for Grasp Synthesis with Multifingered Robot Hand," *The International Conference on Robotics and Automation,* pp. 83–89.

Umetsu, M., and Oniki, K., 1993, "Compliant Motion Control of Arm-Hand System," *JSME International Conference on Advanced Mechatronics,* pp. 429–432.